University of São Paulo
"Luiz de Queiroz" College of Agriculture

Mechanistic numerical modeling of solute uptake by plant roots

Andre Herman Freire Bezerra

Thesis presented to obtain the degree of Doctor of Science. Area: Agricultural Systems Engineering

Piracicaba
2014

Andre Herman Freire Bezerra
Bachelor in Agronomy

Mechanistic numerical modeling of solute uptake by plant roots

Supervisor:
Prof. Dr. **QUIRIJN DE JONG VAN LIER**

Thesis presented to obtain the degree of Doctor of
Science. Area: Agricultural Systems Engineering

Piracicaba
2014

Ao passado,

ao presente e

ao futuro

Com amor, ***DEDICO***

ACKNOWLEDGEMENT

CONTENTS

8

ABSTRACT

Mechanistic numerical modeling of solute uptake by plant roots

Keywords:

RESUMO

Modelagem numérica de extração de solutos pelas raízes

Palavras-chave:

LIST OF FIGURES

14

LIST OF TABLES

16

LIST OF ABREVIATIONS

NU – No solute uptake model

CU – Constant solute uptake model

LU – Linear solute uptake model

NLU – Nonlinear solute uptake model

MM – Michaelis-Menten

LIST OF SYMBOLS

a_i – Tridiagonal matrix coefficient

b_i – Tridiagonal matrix coefficient

c_i – Tridiagonal matrix coefficient

f_i – Tridiagonal matrix coefficient

C – Solute concentration in soil water (mol cm^{-3})

C_0 – Solute concentration in soil water at root surface (mol cm^{-3})

C_{lim} – Limiting solute concentration for potential solute uptake (mol cm^{-3})

C_{min} – Minimum solute concentration where the uptake is zero (mol cm^{-3})

C_2 – Solute concentration threshold for active uptake (mol cm^{-3})

C_{ini} – Initial solute concentration in soil water (mol cm^{-3})

CL – Solute concentration in soil water for linear model (mol cm^{-3})

CNL – Solute concentration in soil water for nonlinear model (mol cm^{-3})

D – Effective diffusion-dispersion coefficient (m^2 s^{-1})

$D_{m,w}$ – Diffusion coefficient in water (m^2 s^{-1})

$diff$ – Difference between linear and nonlinear models for concentration (mol cm^{-3}) and cumulative uptake (mol)

H – Total head (m)

h – Pressure head (m)

h_π – Osmotic head (m)

h_{lim} – Limiting pressure head (m)

I_m – Coefficient of Michaelis-Menten equation (plant demand for solute) (mol m^{-2} s^{-1})

k – Linear component of Michaelis-Menten equation for high concentrations (–)

K – Hydraulic conductivity (m s^{-1})

K_m – Coefficient of Michaelis-Menten equation (plant affinity to the solute type) (mol cm^{-3})

K_s – Saturated hydraulic conductivity (m s^{-1})

L – Root length density (m)

n – Empirical parameter of van Genuchten (1980) (–, in Section XXX) equation or number of elements of the discretized domain (–, in Section XXX)

q – Water flux density (m s^{-1})

q_0 – Water flux density at root surface (m s^{-1})

q_s – Solute flux density (mol m^{-2} s^{-1})

q_{s0} – Solute flux density at root surface (mol m^{-2} s^{-1})

r – Distance from axial center (m)

r_0 – Root radius (m)

r_m – Half distance between roots (m)

t – Time (s)

T_p – Potential transpiration (–)

T_r – Relative transpiration (–)

α – Empirical parameter of van Genuchten (1980) equation (m^{-1})

β – Passive uptake slope (m s^{-1})

Δr – Space step (m)

Δt – Time step (s)

θ – Soil water content (m^3 m^{-3})

Θ – Effective saturation (–)

θ_r – Residual water content (m^3 m^{-3})

θ_s – Saturated water content (m^3 m^{-3})

λ – Empirical parameter of van Genuchten (1980) equation (–)

τ – Solute dispersivity (m)

ψ – Active uptake slope (m s^{-1})

1   INTRODUCTION

Analytical models of transport of nutrients in soil towards plant roots usually consider steady-state conditions with respect to water flow to deal with the high nonlinearity of soil hydraulic functions. Several simplifications (assumptions) are made regarding the uptake of the solutes by the roots, most of them also imposed by the nonlinearity of the influx rate function. Consequently, although the analytical models describe the processes involved in the transport and uptake of solutes, they are capable to simulate water and solute flow just for specific boundary conditions (simplified scenarios that most of the time disagree with real field condition). Therefore, their use in situations that they were not designed for can be a rough approximation. Even being analytical solutions they include special functions (bessels, airys or infinite series, for example) that need, at some point, numerical algorithms to compute results. Thus, for the case of convection–diffusion equation, even the fully analytical solutions are restricted by numerical procedures although they have yet fast and reliable results.

Numerical modeling, in turn, has more flexibility when dealing with nonlinear equations, being an alternative to avoid boundary condition problems. The functions can be solved considering transient conditions for water and solute flow but with some pullbacks like a greater concern about stability and higher time demanded to calculations. In general, numerical models use empirical functions in the determination of osmotic stress, related to the electric conductivity in the soil solution. The parameters of these empirical models depend on soil, plant and atmospheric conditions in a range covered by the experiments that were made to generate data for the model calibration. One must be aware that the use of such models for different scenarios can result in prediction errors not considered by the model itself and, most of the time, new calibration of the parameters needs to be done. A model that uses a mechanistic approach for the solute transport equations can describe the involved processes in a wider range of situations since it is not dependent on experimental data, resulting in a more realistic solution.

In this thesis, a numerical mechanistic solution for the equation of convection–dispersion is developed, assuming a soil concentration dependent solute uptake function as the boundary condition at root surface. The proposed model is compared with a no solute uptake and a constant solute uptake numerical models, and with an analytical model that uses steady-state condition for water content.

2 LITERATURE REVIEW

2.1 Water movement in the soil

(A SHORT INTRODUCTION HERE)

Henry Darcy, in the middle of the 19th century, realized a series of experiments to study the flow of water through a saturated soil within a vertical column, which resulted in the equation

$$Q = K_s A \frac{\Delta H}{L} \tag{1}$$

known as Darcy's law. Q $[\text{L}^3\text{T}^{-1}]$ is the water flow, A $[\text{L}^2]$ is the cross-section area of the column, ΔH $[\text{L}]$ is the difference between the hydraulic potentials at the beginning and the end of the column with length L $[\text{L}]$ and K_s $[\text{LT}^{-1}]$ is a proportionality factor called saturated hydraulic conductivity (LIBARDI, 2010). The Darcy's law is valid for a homogeneous and isotropic soil with a constant cross-section area of the column through its length. Although it is an empirical equation, it can be derived from the relationship between Bernoulli and Poiseuille's laws. For this derivation, see Warrick (2003).

The water flux density q $[\text{LT}^{-1}]$ (also called Darcian velocity) represents the volumetric water flow per unit area and can be generalized to represent the flow in the three spacial dimensions by its differential form (HILLEL, 2003, WARRICK, 2003, LIBARDI, 2005) (commonly used in macroscopic models). It also can represents the flow in radial coordinates (most used in microscopic models), as follows:

$$q = -K_s \frac{dH}{dr} \tag{2}$$

The negative sign arises to determine the direction of the flux, from high to low hydraulic potentials.

The Darcy's law is valid only for laminar flow. The flux (or velocity) q eventually becomes nonlinear as the hydraulic gradient is too high or too low (Figure 1). These deviations can be either attributed to turbulent flow, for high gradients, or to the non-Newtonian behavior of water, for low gradients (HILLEL, 2003; WARRICK, 2003). Notwithstanding the limitations of Darcy's law, it can be applied in the vast majority of cases referring to water flow in soils.

Figure 1 - Darcy's law deviations at high and low fluxes. The continuous line is the actual flux and the dashed lines the Darcy's flux

Source: Adapted from Hillel (2003)

$$\frac{\partial \theta}{\partial t} = -\frac{\partial q}{\partial r}$$

$$\frac{\partial \theta}{\partial t} = \frac{\partial}{\partial r}\left(K(\theta)\frac{\partial h}{\partial r}\right)$$

2.2   Solute availability and transport in soil

Solutes are present in the three phases of the soil. They are adsorbed on the soil colloids (solid), diluted in soil water (liquid) and vaporized in the soil air (gas). Solute transportation between the three phases is constantly occurring in the search for an equilibrium in the soil-plant-atmosphere dynamic system. Although the exchange between the gas phase to the others is important, most of the transport is done by the interaction between solid and liquid phases. As the concentration of ions in soil solution is diminished, due to root extraction or leaching, they are rapidly replenished by the ones that are adsorbed in soil colloids (TINKER; NYE, 2000). Concentration of ions in soil solution is more affected by soil water content than the concentration of adsorbed ions. In a soil with calcium as the predominant cation in the soil solution, for example, a reduction by half of water content practically double its concentration in soil solution. The adsorbed concentration of calcium is slightly changed and it is usually neglected. Roots are only able to take up solutes that are within the soil solution although some authors believe that growing roots that eventually intercept adsorbed solutes on soil colloids can absorb them without water as an intermediate (MARSCHNER; MARSCHNER, 2012). The relation

between adsorbed and solution ion concentration is crucial in determining the ability of the soil to maintain the solution concentration and its mobility.

Solutes in the soil solution must be transported to the root surface to be taken up by the plants. The physic mechanisms involved in this process are diffusion and convection. Similarly as with water, the diffusive solute flow (F_d) within the soil is driven by a gradient (dC/dr) between the root and the surrounding soil, being proportional to the solute diffusivity (D_m), as follows:

$$F_d = -D_m \frac{dC}{dr}$$

It is possible to analytically determine the diffusion of a solute in plain water at a given temperature. It depends on the hydrated radius of the ion.

The coefficient D_m for the diffusive transport is most known as molecular diffusion. The diffusion process results from the random thermal motion of ions or molecules and depends on the temperature and the components of the molecule. As the process of diffusion is occurring in soil, some empirical models (BRESLER, 1973; PAPENDICK; CAMPBEL, 1973) can estimate it by relating to the one of water, as proposed by Millington and Kirk (1961):

$$D_m = \xi D^0 = \frac{\theta^{\frac{10}{3}}}{\theta_s^2} D^0$$

The diffusion coefficient is also affected by the convective flow, thus, to the molecular diffusion, is added a mechanical dispersion coefficient (D_s) which varies with the water flux and soil micropore size. An example of the estimation of the dispersion coefficient is given by (Bear, 1972):

$$D_s = \tau \frac{q}{\theta}$$

Thus, for the overall diffusion processes, a called effective diffusion coefficient is defined as being the sum of both molecular diffusion and molecular dispersion in the general equation of solute flux

$$D = D_m + D_s$$

The mechanical dispersion becomes more important to diffusion as high is the water flux

Figure 2 - Molecular diffusion and mechanical dispersion coefficients as a function of water flux

The soil water content, the interaction of the solute with soil colloids and the distance it must overcome to arrive at the root surface are the main factors governing the diffusion mechanism (WILD et al., 1981). The additional convective component is driven by mass flow of water proportional to the solute concentration, and together with the plant transpiration rate, determines the quantity of ions transported through this mechanism (BARBER, 1974). The predominant mechanism for solute transport depends mainly on the interaction between water and solute uptake rates. At high transpiration rates, mass flow is the primary mechanism of transport. In a case of plant demand for solute is less than the solute flux towards the roots, solute would accumulate at root surface leading to a diffusion of solutes away from the roots (in the opposite direction to the mass flow) until an equilibrium is achieved. In the opposite case, the convective flow towards the roots would be insufficient to meet plant demand for solute and diffusion would become the complementary mechanism (or even more important than convection) of solute transport. It is clear to perceive that diffusion and convection occur simultaneously and, therefore, the solution for the governing equation of solute transport has to deal with both components as two synergic processes.

2.3 Nutrient uptake by plant roots

Once solutes are transported to the root surface, they are readily available to be taken up by the plants. The rate of solute uptake by plant roots can be referred to be similar to that between enzyme and its substrate, described by the Michaelis-Menten (MM) equation (MICHAELIS; MENTEN, 1913). The most well-known form of the equation is the following:

$$I = \frac{I_m C}{K_m + C} \tag{3}$$

where I is the rate of solute uptake, I_m is the maximum uptake rate, C is the solute concentration in the external medium and K_m the Michaelis-Menten constant. I_m is found experimentally and K_m is adjusted as the concentration at which I_m assumes half of its value, and represents the affinity of the plant for the solute. The uptake rate following the MM kinetics is an asymptote which saturates with increasing external concentration (Figure 4). The equation shows that, for very low concentration values ($C \ll K_m$), the uptake rate is proportional to concentration whereas, for $C \gg K_m$, the solute uptake rate is maximal and independent of concentration. Johnson and Goody (2011) revisited the original MM paper and, using modern computer techniques (inexistent by the time the equation was developed), they could get the same results as of the original paper—with no simplifying assumptions—showing how precise and careful was the measurements and equation development. They stressed that the constant found by Michaelis and Menten is I_m/K_m rather than the widely referred K_m.

Epstein and Hagen (1952) were the first to use the MM equation to represent the uptake of a solute and its concentration in external medium (for potassium and sodium solutions in barley roots) and it has been frequently used since then. It describes well the solute uptake for both anions (EPSTEIN et al., 1972, SIDDIQI et al., 1990, WANG et al., 1993) and cations (KOCHIAN; LUCAS, 1982; KELLY; BARBER, 1991; SADANA et al., 2005; BROADLEY et al., 2007; LUX et al., 2011) in the low concentration range and, adding a linear component (k) to the equation, it can properly estimates the uptake rate also for high concentrations (EPSTEIN et al., 1972; KOCHIAN; LUCAS, 1982; BORSTLAP, 1983; WANG et al., 1993; VALLEJO; PERALTA; SANTA-MARIA, 2005; BROADLEY et al., 2007). Many authors agree that for low concentration in external medium, the uptake is driven by an active mechanism of the plant, as it occurs against the solute gradient between root and soil, known as Epstein's mechanism I. For the high concentration range, solutes are freely transported from soil to roots by diffusion and occasional convection. This passive transport is known as Epstein's mechanism II (KOCHIAN; LUCAS, 1982; SIDDIQI et al., 1990). Moreover, experiments have shown that a minimum concentration value (C_{min}) in which the uptake ceases to occur is often found (MOUAT, 1983; DUDAL; DUDAL; ROY, 1995; MACHADO; FURLANI, 2004). Details on Epestein's mechanisms and its physiological processes, and on active and passive uptake, are found on Epstein (1960) and Fried and Shapiro (1961).

The values of MM parameters are strongly dependent on the experimental methods used and vary with plant species, plant age, plant nutritional status, soil temperature

and pH (BARBER, 1995, SHI et al., 2013). Therefore, they have to be determined for each particular experimental situation. Some types of experiments to determine the kinetic parameters I_m, K_m and C_{min} include hydroponically-grow plants (BARBER, 1995) and the use of radioisotopes to estimate them directly from soil (NYE; TINKER, 1977). The latter is more realistic since there is a large difference between a stirred nutrient solution and the complex and dynamic soil medium. Measuring C_{min} is particularly difficult (SEELING; CLAASSEN, 1990; LAMBERS; CHAPIN III; PONS, 2008) because it occurs at very low concentration levels, being hard to be detected. Seeling and Claassen (1990) shows that C_{min} can be neglected for the cases of high K_m values.

Therefore, the MM equation can be often found in a modified form which considers both the linear component and the concentration where uptake is zero, as follows:

$$I = \frac{I_m(C - C_{min})}{K_m + C - C_{min}} + k(C - C_{min}) \tag{4}$$

The addition of the new parameters changes the solute uptake rate as shown in Figure 3. By the fact that the solute uptake rate acts in distinct ways for different solute concentration ranges, the modified MM equation may be considered a stepwise function.

Both the original and the modified MM equation have been used in numerical (NYE; MARRIOTT, 1969, SILBERBUSH; BEN-ASHER; EPHRATH, 2005, ŠIMUNEK; HOPMANS, 2009, BECHTOLD et al., 2011) and analytical (BARBER, 1995; ROOSE; FOWLER; DARRAH, 2001) solute uptake models. Authors do not agree on which cases one equation has to be chosen over the other, it all depends on the assumptions made for each particular model. During the history of the development of nutrient uptake models—using MM equation—some authors have used the modified version to estimate both passive and active uptake while others have chosen the original one to deal with active uptake only (SHI et al., 2013).

Figure 3 - Solute uptake rate as a function of external concentration. The saturable component is the first term of the right-hand side of Eq. (4), the linear component is the second term and the total uptake is Eq. (4) itself

There are other alternatives to describe the solute uptake rate function apart from MM equation. Dalton, Raats and Gardner (1975) proposed a physical-mathematical model that include active uptake, mass flow and diffusion, and express solute uptake as being proportional to root water uptake. Bouldin (1989) described the uptake from low and high concentrations solutions by two linear equations, simplifying the process of solute uptake at root surface to two diffusion components. Nye and Tinker (1977) determined the uptake rate as a linear component followed by a constant rate phase where the threshold value is dependent on solute concentration inside the plant. Nevertheless, MM equation is yet the mostly used equation in root solute uptake models for being physically grounded and for its good agreement with experimental data.

2.4   Transpiration reduction functions for water and solute

2.5   Water and solute uptake models

3 THEORETICAL FRAMEWORK (base, foundations)

This chapter focuses on the theoretical aspects used in the methodology. It briefly describes the Richards equation that is applied in water flow models and details the convection-dispersion equation for solute transport. Also, a short explanation about the Michaelis-Menten kinetics for nutrient uptake is given. For those who are familiarized with these theories, the reading starting from Chapter 4 is sufficient and this chapter may be skipped, since it does not provide any particular information that is different from what is already known from literature. Equations that were presented in this section, and are used further in this thesis, are properly referenced.

3.1 Water flow equation

The equation for water flow for a homogeneous and isotropic soil, in saturated and non-saturated conditions, is given by the Richards equation. In radial coordinates, it can be written as:

$$r\frac{\partial \theta}{\partial t} = -\frac{\partial q}{\partial r} \tag{5}$$

where r (m) is the distance from the root axial center, θ (m^3 m^{-3}) is the water content in soil and t (s) is the time. The water flux density q (m s^{-1}) is given by the Darcy-Buckingham equation:

$$q = -K(\theta)\frac{dH}{dr} \tag{6}$$

where K (m s^{-1}) is the soil hydraulic conductivity and H is the total hydraulic potential. This equation describes the laminar water flux for (non)saturated soil in any direction of space.

Equation (5) is a second-order partial differential equation and, therefore, needs initial and boundary conditions to result in a particular solution. The most common initial condition is of constant water content or pressure head along the radial distance, although a function of water content (or pressure head) over distance can also be used. In analytical solutions, steady-state condition in relation to water flow is often used to solve the equation. The high non-linearity of the hydraulic functions (see Section 3.2) makes a transient solution rather complex and, sometimes, impractical. In numerical solutions, on the other hand, it is easier to define a transient water flow condition, which gives a more realistic treatment to the equation. Boundaries for both steady-state and transient

solutions can be either of prescribed pressure head or water flux, as shown in Equations (7) and (8) respectively:

$$h(r_i, t) = f(t) \tag{7}$$

$$K(\theta)\frac{\partial h}{\partial r}\bigg|_{r=r_i} = g(t) \tag{8}$$

where $f(t)$ and $g(t)$ can be either a constant or a time variable function of pressure head and water flux, respectively; and r_i is the distance from axial center to the specific boundary. In the case of microscopic (and usually radial) models, r_i can assume values of distance from axial center to root surface (inner boundary) and to the end of the domain (outer boundary). Macroscopic models use the Cartesian system and, for one-dimension, represents the domain along the z axis (depth) instead of r. Thus, z_i values would be of the distance from the soil surface (top boundary) to a certain depth, *e.g.* root depth (bottom boundary).

In most of microscopic (single root) models, the boundary conditions are of flux type, according to Equation (8). At root surface, it is equal to the transpiration rate, and at the outer boundary, it is often of zero flux — meaning inter-root competition for water. Therefore, the only water exit is at root surface through the transpiration stream. In macroscopic models, as they deal with the entire root zone, both boundary types are equally found, depending on the simulation scenario to consider (soil surface evaporation, irrigation or rain, presence of water table, drainage, water root uptake, etc.). A sink-source term is then added to Equation (5) to deal with such water inputs and outputs (as seen in the previous chapter).

The hydraulic potential H is the sum of pressure (h) and elevation (h_g) heads in models that do not consider solute flow. In order to deal with solutes, the osmotic head (h_π) must be added to H and it will serve as a 'link' to the solute transport equation, detailed in Section 3.3. Moreover, h_g can be neglected when this component is of minor relevance (as of in microscopic models).

3.2 Soil hydraulic functions

The soil hydraulic properties K, θ and h are interdependent and, as mentioned in the previous section, highly nonlinear. Equations (9) and (10) show their interdependence and their noticeable nonlinearity. Among all models to describe the water retention curve mentioned in Chapter 2, the most used is the one of van Genuchten below:

$$\theta(h) = \theta_r + \frac{\theta_s - \theta_r}{[1 + |\alpha h|^n]^{1-(1/n)}} \tag{9}$$

$$K(\theta) = K_s \Theta^\lambda [1 - (1 - \Theta^{n/(n-1)})^{(1-(1/n))}]^2 \tag{10}$$

where Θ $(-)$ is the effective saturation defined by $\frac{(\theta-\theta_r)}{(\theta_s-\theta_r)}$; θ_s (m^3 m^{-3}) and θ_r (m^3 m^{-3}) are the saturated and residual water contents, respectively; and α (m^{-1}), λ $(-)$ and n $(-)$ are empirical parameters.

Luckily, the relationship between the hydraulic functions allows to determine a property as a function of another. Thus, by measuring two of them, it is possible to fit the parameters of Equations (9) and (10). A common practice is to measure θ at prescribed values of h and adjust the Equation (9) parameters with the data, consequently obtaining the K function.

3.3 Solute transport

The solute transport in soil occurs by diffusion and convection. The equation that involves those mechanisms is the convection-diffusion equation. In radial coordinates, it can be written as:

$$r\frac{\partial(\theta C)}{\partial t} = -\frac{\partial q_s}{\partial r} \tag{11}$$

where C (mol cm^{-3}) is the concentration of solute in soil solution. The solute flux density q_s (mol m^{-2} s^{-1}) is given by:

$$q_s = -D(\theta)\frac{dC}{dr} + qC \tag{12}$$

where D (m^2 s^{-1}) is the effective diffusion-dispersion coefficient. This equation describes the solute flux in the soil solution. The convective flux is accounted by the second term on the right-hand side of the equation (12) and the diffusive-dispersive flux by the first term.

Transport by convection occurs due to movement of diluted solutes carried by mass flow of water proportional to the solute concentration in soil solution. It is noticeable that the convective contribution to solute flux reduces as water flux q becomes small, therefore the convective flux is highly dependent on water content gradient and hydraulic conductivity. Convection also affects the solute diffusivity due to a water velocity gradient originated in the micropore space of the soil. As solutes are carried with different velocities, a concentration gradient is originated, allowing a diffusive movement within this pore space. This microscale process is called mechanical dispersion and can be expressed by macroscopic variables as follows:

$$D_s = \tau \frac{q}{\theta} \tag{13}$$

where D_s (m^2 s^{-1}) is the mechanical dispersion coefficient, τ (m) is the dispersivity and the relation q/θ (m s^{-1}) accounts for the average pore water velocity.

Transport by diffusion is the movement of solutes caused by a concentration gradient in soil solution. It is proportional to the effective diffusion coefficient D which is given by:

$$D = D_m + D_s \tag{14}$$

where D_m (m^2 s^{-1}) is the molecular diffusion coefficient that, as D_s, is also a microscale process resulted from the averaged random motion of the molecules in the soil solution in response to the concentration gradient. It can be expressed by macroscopic variables as follows:

$$D_m = \xi D^0 = \frac{\theta^{\frac{10}{3}}}{\theta_s^2} D^0 \tag{15}$$

where ξ (–) is the tortuosity factor and D^0 (m^2 s^{-1}) is the diffusion coefficient in water. Values of D^0 for ions or molecules can be easily measured and estimated by analytical equations for free water. Soil water content is often below its saturation point, thus, diffusion is often different from that of free water. Equations (13) to (15) are one of the several existing models to estimate the effective diffusion-dispersion coefficient. Chapter 2 has a list of the available models.

The boundary conditions types are the same as of water, except that they are in respect to concentration instead of pressure head. In microscopic models, common boundary conditions are of zero, constant or variable solute flux at root surface. Choosing

one over another depends on how the solute uptake by the plant will be considered in the model (details in Section 3.4). The outer boundary depends on the distance in which it is considered. A zero solute flux condition works well to simulate inter-root competition for solutes in a distance ranging from XXX to xxx m while constant concentration — equal to the initial concentration — can be used in a situation that the boundary is 'far enough' from root surface, *i.e.* there is no competition between neighbour roots. In macroscopic models, a sink-source term is added to Equation (11) to consider different inputs and outputs of solute in the system (*e.g.* plant uptake, mineralization, degradation, etc.), and the top and bottom boundaries are treated according to the scenario (similar to what is done with the water flow equation).

3.4 Solute uptake by plant roots

The transition from fluxes of water and solutes in the soil to physiological mechanisms of uptake by the plant is located at the root-soil interface. This boundary is of the outermost importance and a correct mathematical treatment here is crucial. Different conditions in this boundary result in distinct solutions of the convection-dispersion equation and, consequently, lead to different results. For a situation of zero solute flux at root surface, the solute would accumulate in that region due to the transport by convection. A consequent diffusion of solutes away from the root would occur due to the formed concentration gradient until an equilibrium between those fluxes is achieved. On the other hand, considering a constant or a variable solute flux at root surface, an accumulation of solute would occur uniquely if the root uptake is less than the solute flux arriving at root surface. The opposite situation would cause a decrease in concentration at root surface until a zero (or limiting) concentration value.

Writing the convection-diffusion equation in its full form, by substituting Equation (12) in Equation (11) as

$$r\frac{\partial(\theta C)}{\partial t} = \frac{\partial}{\partial r}\left(D(\theta)\frac{\partial C}{\partial r} - qC\right) \tag{16}$$

and with a flux type boundary condition at root surface of

$$-D(\theta)\frac{\partial C}{\partial r}\bigg|_{r=r_0} + qC = F \ , \tag{17}$$

all conditions of solute uptake rate can be represented by setting to F a specific uptake function. A zero solute uptake condition would be $F = 0$, a constant uptake condition

would be $F = k$ and a concentration dependent uptake function would be $F = \alpha(C)k$, where k (mol m^{-2} s^{-1}) is a constant that represents the uptake rate and $\alpha(C)$ (–) a shape function for the uptake.

The rate of solute uptake by plant roots can be referred to be similar to that between enzyme and its substrate, described by the Michaelis-Menten (MM) equation (MICHAELIS; MENTEN, 1913). Thus the uptake shape function $\alpha(C)$ can follow the concentration dependent MM kinetics, and k being equal to I_m leads to the following:

$$\alpha(C) = \frac{C}{K_m + C} \Rightarrow F = \frac{C}{K_m + C} I_m \tag{18}$$

where I_m is the maximum uptake rate, C is the solute concentration in soil solution and K_m the Michaelis-Menten constant. I_m is found experimentally and K_m is adjusted as the concentration at which I_m assumes half of its value, being interpreted as the affinity of the plant for the solute.

The uptake rate following the MM kinetics is an asymptote which saturates with increasing external concentration (Figure 4). The equation shows that, for very low concentration values ($C \ll K_m$), the uptake rate is proportional to concentration whereas, for $C \gg K_m$, the solute uptake rate is maximal and independent of concentration.

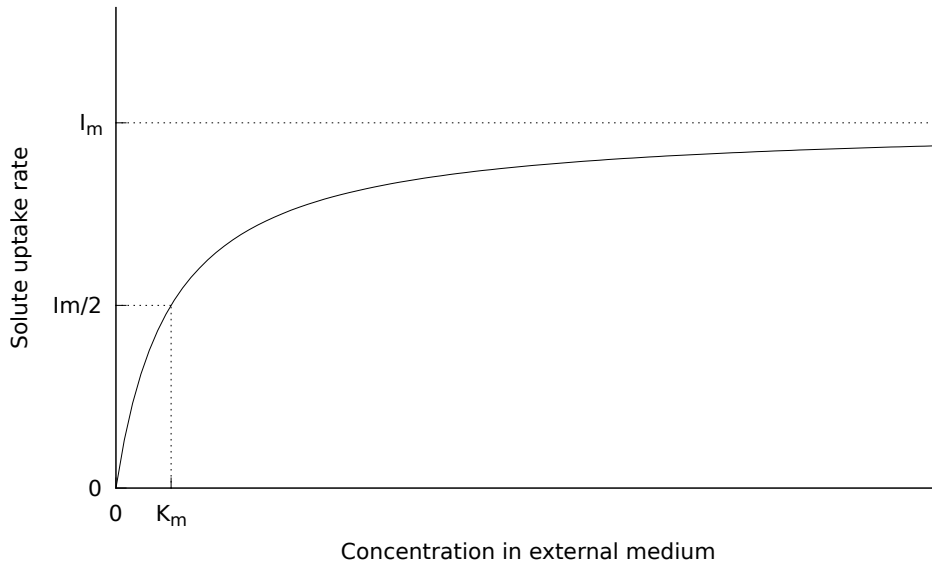Figure 4 - Solute uptake rate as a function of external concentration following Michaelis-Menten kinetics with its more common parameters

The K_m coefficient represents the affinity of the plant for the solute. For K_m values higher than 50 μM, it is considered that the plant has a low affinity for the solute whereas for values less than 10 μM, the plant has a high-affinity for it.

4 METHODOLOGY

To get the desired results of solute concentration as a function of time and radial distance from the axial center, as well to compute the total amount of solute extracted by the plant in a prescribed time, a fully implicit numerical treatment was given to the Equations (5) and (11), that accounts for water and solute flow, respectively. For any numerical solution, the pace and time domains must be discretized in order to calculate the results for each 'piece of space and time'. Our system domain is a single root (microscopic model) that are competing for water and solute with its neighbours in a homogeneous and isotropic soil... (MORE ABOUT THE MODEL). Figure 5 shows a schematic representation of the domain considered in the simulations.

The equations for water and solute flow ((5) and (11), respectively) were solved using a fully implicit numerical scheme. The model here presented is microscopic with radial geometry, in a homogeneous and isotropic soil, with one ion only soil solution. The water and solute flow are axis-symmetric. The schematic representation of the discretized domain is shown in Figure 5.
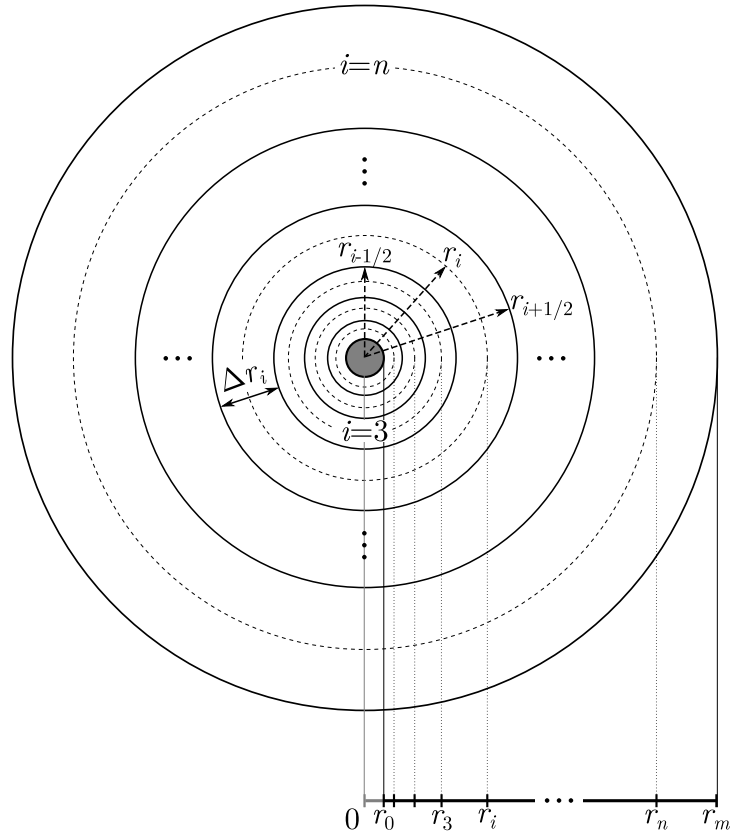
Figure 5 - Schematic representation of the discretized domain considered in the model

Figure 6 - Schematic representation of the spatial distribution of roots in the root zone

The solute uptake boundary condtition is this study was choosen to follow the MM kinetics equation assuming the original equation, without C_{min} and linear term for hig concentration solutions as being active and passive as being the convective transport of solute, by mass flow of water.

Active uptake happens here only in low concentrations. For cases with C_{lim} happens in high concentration, the numerics did not converged, maybe for the use of a fully implicit numerical method and/or for not taking into account the linear term of MM equation.

The linearization proposed in the model is very si,ilar to that of Tinker and Nye (pg.116)

Here is explained how water flow and solute transport equations were solved with its respective assumptions and boundary conitions, as well as the methodology in the comparisson for the linear and nonlinear uptake rate cases and the comparissons with the other solute uptake models.

The partial differential equations for water movement and solute transport in soil are solve numerically in a fully implicit way. Both water and solute flow are considered to have transient condition.

The water and solute differential equations for one-dimensional axisymetric flow were solved numerically and simulated iteratively as described in the following. The algorithm was based on the solution proposed by de Jong van Lier, Metselaar and van Dam (2006) and de Jong van Lier, van Dam and Metselaar (2009).

4.1 Water movement equation

USE IT: In this thesis, we will consider H as being the sum of pressure and osmotic heads (h and h_π, respectively) since the gravitational component can be neglected due to the scale of the chosen domain (region around a single root with XXX m^2).

The Richards equation for one-dimensional axisymetric flow, assuming no sink or source and no gravitational component, can be written as:

$$\frac{\partial \theta}{\partial H} \frac{\partial H}{\partial t} = \frac{1}{r} \frac{\partial}{\partial r} \left(rK \frac{\partial H}{\partial r} \right) \tag{19}$$

where θ (m^3 m^{-3}) is the water content, H (m) is the sum of pressure (h) and osmotic (h_π) heads, t (s) is the time, r (m) is the distance from the axial center and K (m s^{-1}) is the hydraulic conductivity.

Relations between K, θ and h are described by the van Genuchten equation system:

$$\Theta = [1 + |\alpha h|^n]^{(1/n)-1} = \frac{(\theta - \theta_r)}{(\theta_s - \theta_r)} \tag{20}$$

$$K = K_s \Theta^\lambda [1 - (1 - \Theta^{n/(n-1)})^{(1-(1/n))}]^2 \tag{21}$$

where θ_r and θ_s (m^3 m^{-3}) are residual water content and saturated water content, respectively; α (m^{-1}), n and λ are empirical parameters.

4.1.1 Boundary conditions for water movement equation

4.2 Solute transport equation

The differential equation for convection-dispersion for transient one-dimensional axisymetric flow can be written as:

$$r \frac{\partial(\theta C)}{\partial t} = -\frac{\partial}{\partial r} \left(rqC \right) + \frac{\partial}{\partial r} \left(rD \frac{\partial C}{\partial r} \right) \tag{22}$$

where C (mol m^{-3}) is the solute concentration in the soil solution, q (m s^{-1}) is the water flux density and D (m^2 s^{-1}) is the effective diffusion-dispersion coefficient.

4.2.1 Michaelis-Menten equation

The solute flux density at root surface (q_{s0}) can be related to the Michaelis-Menten (MM) equation as the following:

$$q_{s0} = -D\frac{dC}{dr} + q_0 C \simeq \frac{I_m C_0}{K_m + C_0} + q_0 C_0 \qquad (23)$$

where D (m^2 s^{-1}) is the effective diffusion-dispersion coefficient; q_0 (m^2 s^{-1}) is the water flux density at the root surface; I_m (mol m^2 s^{-1}) and K_m (mol m^{-3}) are the MM parameters that represent the maximum solute uptake rate and the affinity of the plant to the solute type, respectively; and C_0 (mol m^{-3}) is the solute concentration in the soil solution at root surface.

We assume that the diffusive and convective parts of the original equation is similar to the active and passive uptakes of the MM equation, respectively, at root suurface. It is shown in Figure 0 XXX the two proposed partitioning of active and passive uptakes, for a constant water flux density. Figure 0a is linear, which is a simplification of MM equation to facilitate its use in the numerical solution. Figura 0a is the MM equation itself.

Figure 7 - Uptake (influx) rate as a function of concentration in soil water for [a] nonlinear case and [b] linear case

In the linearized equation (Figure 0b), the slope β of the total uptake line (continuous line), for concentration values smaller than C_{lim}, can be found by the relation $I_m/Clim$, since the line starts at the origin. According to the MM equation, for values smaller than C_{lim}, the solute uptake is concentration dependent and the uptake is smaller

than I_m. For values greater than C_2 the uptake is also concentration dependent but due to transport of mass by water flow only, i.e, active uptake is zero and the overall uptake is passive.

To find C_{lim}, we set the solute flux density to I_m:

$$I_m = \frac{I_m C_0}{K_m + C_0} + q_0 C_0 \ . \tag{24}$$

Solving for C, we find C_{lim} as the positive value of:

$$C_{lim} = -\frac{K_m \pm \left(K_m{}^2 + 4I_m K_m/q_0\right)^{1/2}}{2} \tag{25}$$

Finally, β can be defined as the positive value of:

$$\beta = -\frac{I_m}{C_{lim}} = -\frac{2I_m}{K_m \pm \left(K_m{}^2 + 4I_m K_m/q_0\right)^{1/2}} \tag{26}$$

At concentration values greater than C_2, the solute uptake is driven only by mass flow of water and the active uptake is zero. Thus, C_2 can be found as:

$$C_2 = \frac{-I_m}{q_0} \tag{27}$$

The partitioning between active (α) and passive uptake (q_0) is done by difference, as the values of total uptake and passive uptake is always known:

$$q_{s0} = (\text{active slope} + \text{passive slope})\, C_0 = \beta\, C_0$$
$$\text{passive slope} = q_0$$
$$\text{active slope} = \beta - q_0 = \alpha$$
$$q_{s0} = (\alpha + q_0)\, C_0 \tag{28}$$

The equation (28) is, therefore, the linearization of equation (23) for values of concentration smaller than C_{lim} and greater than C_2.

4.2.2 Boundary conditions for solute transport equation

The solute flux density at the outermost compartment (half distance between roots, i.e., $r = r_m$) is set to zero. The boundary conditions at innermost compartment (root surface, i.e, $r = r_0$) are set according to the model type, which are: no solute uptake model (de Jong van Lier, 2009), constant uptake model (de Willigen, 1994) and linear and nonlinear concentration–dependent model (proposed). For short, let us call them NU, CU, LU and NLU models, respectively.

For no solute uptake (NU) model type: the solute flux density is set to zero

$$q_{s0} = -D\frac{dC}{dr} + q_0 C = 0 \tag{29}$$

For constant solute uptake (CU) model type: the solute flux density is set to the maximum and constant solute uptake rate I_m. For cylindrical coordinates, the solute flux density of each root is

$$q_{s0} = -D\frac{dC}{dr} + q_0 C = -\frac{I_m}{2\pi r_0 L} \tag{30}$$

where L (m) is the root length, r_0 (m) is the root radius and I_m has units of mol s^{-1}.

For linear concentration–dependent uptake (LU) model type: the solute flux density is set to the linearized piecewise MM equation

$$q_{s0} = -D\frac{dC}{dr} + q_0 C = -(\alpha + q_0)C_0 \tag{31}$$

For nonlinear concentration–dependent uptake (NLU) model type: the solute flux density is set to the MM equation

$$q_{s0} = -D\frac{dC}{dr} + q_0 C = -\left(\frac{I_m}{2\pi r_0 L(K_m + C_0)} + q_0\right)C_0 \tag{32}$$

4.3 Numerical solution

The combined water and salt movement is simulated iteratively. In a first step, the water movement toward the root is simulated, assuming salt concentrations from the previous time step. In a second step, the salt contents per segment are updated and new values for the osmotic head in all segments are calculated. The first step is then repeated with updated values for the osmotic heads. This process is repeated until the pressure head values and osmotic head values between iterations converge. Two flowcharts with the algorithm procedures to solve water and solute iterative equations can be found in the Appendix.

4.3.1 Water

The implicit numerical discretization and the solution for the Eq. (19) was made according to de Jong van Lier et al. (2006), which has the following criteria:

(i) there is no sink (the only water exit is the root surface located at the inner side of the first compartment)

(ii) water flux density at the outermost compartment is set to zero

(iii) water flux density at the innermost compartment (at root surface) is set equal to water flux density entering the root, which is determined by transpiration rate and total root area

4.3.2 Solute

Fully implicit numerical discretization of Eq. (22) gives:

$$\theta_i^{j+1} C_i^{j+1} - \theta_i^j C_i^j = \frac{\Delta t}{2 r_i \Delta r_i} \times$$

$$\left\{ \frac{r_{i-1/2}}{r_i - r_{i-1}} \left[q_{i-1/2}(C_{i-1}^{j+1} \Delta r_i + C_i^{j+1} \Delta r_{i-1}) - 2 D_{i-1/2}^{j+1}(C_i^{j+1} - C_{i-1}^{j+1}) \right] - \right. \tag{33}$$

$$\left. \frac{r_{i+1/2}}{r_{i+1} - r_i} \left[q_{i+1/2}(C_i^{j+1} \Delta r_{i+1} + C_{i+1}^{j+1} \Delta r_i) - 2 D_{i+1/2}^{j+1}(C_{i+1}^{j+1} - C_i^{j+1}) \right] \right\}$$

where $i\,(1 \leq i \leq n)$ is the segment number and j is the time step.

The boundary conditions at the root surface, for solutes, (inner boundary, $i = 1$) will be of zero, constant and concentration dependent solute flux, according to the models of de Jong van Lier (2009), de Willigen (1984) and proposed model, respectively.

The algorithm used in numerical simulations to solve Eq. (33) consist in finding C_i^{j+1} for each segment, which can be done by solving the tridiagonal matrix as follows

$$\begin{bmatrix} b_1 & c_1 & & & & \\ a_2 & b_2 & c_2 & & & \\ & a_3 & b_3 & c_3 & & \\ & & \ddots & \ddots & \ddots & \\ & & & a_{n-1} & b_{n-1} & c_{n-1} \\ & & & & a_n & b_n \end{bmatrix} \begin{bmatrix} C_1^{j+1} \\ C_2^{j+1} \\ C_3^{j+1} \\ \vdots \\ C_{n-1}^{j+1} \\ C_n^{j+1} \end{bmatrix} = \begin{bmatrix} f_1 \\ f_2 \\ f_3 \\ \vdots \\ f_{n-1} \\ f_n \end{bmatrix} \tag{34}$$

with $f_i(\text{mol m}^{-2})$ defined, unless specified otherwise, as

$$f_i = r_i \theta_i^j C_i^j \tag{35}$$

and $a_i\,(\text{m})$, $b_i\,(\text{m})$ and $c_i\,(\text{m})$ are defined according to the respective segments and model type as described in the following.

1. The intermediate nodes ($i = 2$ to $i = n - 1$) are the same for all models

Rearrangement of Eq. (33) to eq. (34) results in the coefficients:

$$a_i = -\frac{r_{i-1/2}(2 D_{i-1/2}^{j+1} + q_{i-1/2} \Delta r_i) \Delta t}{2(r_i - r_{i-1}) \Delta r_i} \tag{36}$$

$$b_i = r_i \theta_i^{j+1} + \frac{\Delta t}{2 \Delta r_i} \left[\frac{r_{i-1/2}}{(r_i - r_{i-1})}(2 D_{i-1/2}^{j+1} - q_{i-1/2} \Delta r_{i-1}) + \right.$$

$$\left. \frac{r_{i+1/2}}{(r_{i+1} - r_i)}(2 D_{i+1/2}^{j+1} + q_{i+1/2} \Delta r_{i+1}) \right] \tag{37}$$

$$c_i = -\frac{r_{i+1/2} \Delta t}{2 \Delta r_i (r_{i+1} - r_i)}(2 D_{i+1/2}^{j+1} - q_{i+1/2} \Delta r_i) \tag{38}$$

2. The outer boundary ($i = n$) is also the same for all models, which is of zero solute flux

Applying boundary condition of zero solute flux, the third and forth term from the right hand side of Eq. (33) are equal to zero. Thus, the solute balance for this segment is written as:

$$\theta_n^{j+1}C_n^{j+1} - \theta_n^j C_n^j = \frac{\Delta t}{2r_n \Delta r_n} \times$$
$$\left\{ \frac{r_{n-1/2}}{r_n - r_{n-1}} \left[q_{n-1/2}(C_{n-1}^{j+1}\Delta r_n + C_n^{j+1}\Delta r_{n-1}) - 2D_{n-1/2}^{j+1}(C_n^{j+1} - C_{n-1}^{j+1}) \right] \right\} \quad (39)$$

Rearrangement of Eq. (39) to Eq. (34) results in the coefficients:

$$a_n = -\frac{r_{n-1/2}(2D_{n-1/2}^{j+1} + q_{n-1/2}\Delta r_n)\Delta t}{2(r_n - r_{n-1})\Delta r_n} \quad (40)$$

$$b_n = r_n \theta_n^{j+1} + \frac{\Delta t}{2\Delta r_n} \left[\frac{r_{n-1/2}}{(r_n - r_{n-1})}(2D_{n-1/2}^{j+1} + q_{n-1/2}\Delta r_{n-1}) \right] \quad (41)$$

3. The inner boundary $(i = 1)$

  a) **Zero (no) uptake model (NU)**

  Applying boundary condition of zero solute flux, the first and second term of the right-hand side of Eq. (33) are equal to zero:

$$\theta_1^{j+1}C_1^{j+1} - \theta_1^j C_1^j = \frac{\Delta t}{2r_1 \Delta r_1} \times$$
$$\left\{ \frac{r_{1+1/2}}{r_2 - r_1} \left[-q_{1+1/2}(C_1^{j+1}\Delta r_2 + C_2^{j+1}\Delta r_1) + 2D_{1+1/2}^{j+1}(C_2^{j+1} - C_1^{j+1}) \right] \right\} \quad (42)$$

  Rearrangement of Eq. (42) to Eq. (34) results in the following coefficients:

$$b_1 = r_1 \theta_1^{j+1} + \frac{\Delta t}{2\Delta r_1} \left[\frac{r_{1+1/2}}{(r_2 - r_1)}(2D_{1+1/2}^{j+1} + q_{1+1/2}\Delta r_2) \right] \quad (43)$$

$$c_1 = -\frac{r_{1+1/2}\Delta t}{2\Delta r_1(r_2 - r_1)}(2D_{1+1/2}^{j+1} - q_{1+1/2}\Delta r_1) \quad (44)$$

  b) **Constant uptake model (CU)**

  Applying boundary conditions of constant solute flux, the first and second term of the right-hand side of Eq. (33) are equal to $-\frac{I_m}{2\pi r_0 L}\Delta r_1$ while $C > 0$:

$$\theta_1^{j+1}C_1^{j+1} - \theta_1^j C_1^j = \frac{\Delta t}{2r_1 \Delta r_1} \times$$
$$\left\{ \frac{r_{1-1/2}}{r_1 - r_0} \left(-\frac{I_m}{2\pi r_0 L} \right) \Delta r_1 - \right. \quad (45)$$
$$\left. \frac{r_{1+1/2}}{r_2 - r_1} \left[q_{1+1/2}(C_1^{j+1}\Delta r_2 + C_2^{j+1}\Delta r_1) - 2D_{1+1/2}^{j+1}(C_2^{j+1} - C_1^{j+1}) \right] \right\}$$

When $C = 0$ the maximum solute flux (I_m) is set to zero and the equation becomes equal to Eq. (42). Rearrangement of Eq. (45) to Eq. (34) results in the following coefficients:

$$b_1 = r_1\theta_1^{j+1} + \frac{\Delta t}{2\Delta r_1}\left[\frac{r_{1+1/2}}{(r_2 - r_1)}(2D_{1+1/2}^{j+1} + q_{1+1/2}\Delta r_2)\right] \tag{46}$$

$$c_1 = -\frac{r_{1+1/2}\Delta t}{2\Delta r_1(r_2 - r_1)}(2D_{1+1/2}^{j+1} - q_{1+1/2}\Delta r_1) \tag{47}$$

$$f_1 = r_1\theta_1^j C_1^j - \frac{r_{1-1/2}}{r_1 - r_0}I_m\frac{\Delta t}{4\pi r_0 L} \tag{48}$$

c) **Linear concentration dependent model (LU)**

Applying boundary conditions of linear concentration dependent solute flux, the first and second term of the right-hand side of Eq. (33) are equal to $-(\alpha + q_0)C_1^{j+1}\Delta r_1$ while $C < C_{lim}$ and $C > C_2$:

$$\theta_1^{j+1}C_1^{j+1} - \theta_1^j C_1^j = \frac{\Delta t}{2r_1\Delta r_1}\times$$
$$\left\{\frac{r_{1-1/2}}{r_1 - r_0}\left[-(\alpha + q_0)\right]C_1^{j+1}\Delta r_1 - \right. \tag{49}$$
$$\left.\frac{r_{1+1/2}}{r_2 - r_1}\left[q_{1+1/2}(C_1^{j+1}\Delta r_2 + C_2^{j+1}\Delta r_1) - 2D_{1+1/2}^{j+1}(C_2^{j+1} - C_1^{j+1})\right]\right\}$$

When $C = 0$ the solute flux is set to zero and the equation is equal to Eq. (42). While $C_{lim} \leq C \leq C_2$, the solute flux density is constant and the equation is equal to Eq. (45). Rearrangement of Eq. (49) to Eq. (34) results in the following coefficients:

$$b_1 = r_1\theta_1^{j+1} + \frac{\Delta t}{2\Delta r_1}\left[\frac{r_{1+1/2}}{(r_2 - r_1)}(2D_{1+1/2}^{j+1} + q_{i+1/2}\Delta r_2) - \frac{r_{1-1/2}}{r_1 - r_0}(\alpha + q_0)\Delta r_1\right] \tag{50}$$

$$c_1 = -\frac{r_{1+1/2}\Delta t}{2\Delta r_1(r_2 - r_1)}(2D_{1+1/2}^{j+1} - q_{1+1/2}\Delta r_1) \tag{51}$$

d) **Nonlinear concentration dependent model (NLU)**

Applying boundary conditions of nonlinear concentration dependent solute flux, the first and second term of the right-hand side of Eq. (33) are equal to $-(\frac{I_m}{2\pi r_0 L(K_m + C_1^{j+1})} + q_0)C_1^{j+1}\Delta r_1$ while $C < C_{lim}$ and $C > C_2$:

$$\theta_1^{j+1}C_1^{j+1} - \theta_1^j C_1^j = \frac{\Delta t}{2r_1\Delta r_1}\times$$
$$\left\{\frac{r_{1-1/2}}{r_1 - r_0}\left[-(\alpha + q_0)\right]C_1^{j+1}\Delta r_1 - \right. \tag{52}$$
$$\left.\frac{r_{1+1/2}}{r_2 - r_1}\left[q_{1+1/2}(C_1^{j+1}\Delta r_2 + C_2^{j+1}\Delta r_1) - 2D_{1+1/2}^{j+1}(C_2^{j+1} - C_1^{j+1})\right]\right\}$$

Rearrangement of Eq. (52) to Eq. (34) results in the following coefficients:

$$b_1 = r_1\theta_1^{j+1} + \frac{\Delta t}{2\Delta r_1}\left[\frac{r_{1+1/2}}{(r_2 - r_1)}(2D_{1+1/2}^{j+1} + q_{i+1/2}\Delta r_2) - \right.$$

$$\left.\frac{r_{1-1/2}}{r_1 - r_0}\left(\frac{I_m}{2\pi r_0 L(K_m + C_1^{j+1})} + q_0\right)\Delta r_1\right] \tag{53}$$

$$c_1 = -\frac{r_{1+1/2}\Delta t}{2\Delta r_1(r_2 - r_1)}(2D_{1+1/2}^{j+1} - q_{1+1/2}\Delta r_1) \tag{54}$$

The value of C_1^{j+1} in Equation (53) is found using the iterative Newton-Raphson method. Note that since this is a one-dimensional microscopic model, it is assumed that the root has the same characteristcs in all vertical soil profile (along its vertical axis), thus, water and solute transport from soil towards the roots and uptakes are occurring at the same rate in the vertical profile. It is possible to couple this model in another one that has discretized soil layers. For a 2D model (depth and radial distance), the solutions presented here are applied in each layer independently. For a 1D model (only depth), an average of water and solute content through the horizontal profile has to be determined.

4.4 Other models

4.5 Analysis of linear and nonlinear approaches

To analyze the differences between the two proposed models (linear and nonlinear), the absolute and relative differences were calculated as follows:

$$diff_{abs} = \sum_{t=1}^{t_{end}}|CL_t - CNL_t| \tag{55}$$

$$diff_{rel} = \frac{\sum_{t=1}^{t_{end}}|CL_t - CNL_t|}{\sum_{t=1}^{t_{end}}CL_t} \tag{56}$$

where CL_t and CNL_t are the solute concentration in soil water for LU and NLU, respectvely, at a given time t, and t_{end} is the end time of the simulation.

The equations are the same of absolute and relative errors but since we are analyzing differences instead of errors (there is not a right or standard model), we called it differences.

This section describes how the linear (LU) and nonlinear (NLU) solutions simulate the transport of water and solutes in the soil, plant and atmosphere system. The

analysis of the results was made in order to choose one out of the two models in further simulations. The nonlinear solution uses the original MM equation but it takes longer to run due to an additional iterative process that has to be made. NLU is also more susceptible to stabilization problems in the results. The linear model is a simplified version of the MM equation in which the solute uptake rate for the situation $C < C_{lim}$ is smaller when compared to the original nonlinear equation, it has no stabilization problems and runs faster. Therefore, the objective of this section is to analyze the differences between the results of the two models and check if those differences are significant. For that, four different general scenarios were chosen (using the parameters listed in Table 2, with loam soil) as listed below:

- Scenario 1: Medium root length density, High concentration and High potential transpiration
- Scenario 2: Medium root length density, High concentration and Low potential transpiration
- Scenario 3: Low root length density, High concentration and High potential transpiration
- Scenario 4: Medium root length density, Low concentration and High potential transpiration

4.5.1 Statistical difference

Also, the Mann–Whitney U test was made with two datasets (concentration and cumulative uptake) for the two models. The choice of this test is due to the fact that the distributions for both datasets are not normal, the pairs (concentration for LU and for NLU and cumulative uptake for LU and NLU) are distinct and do not affect each other. This test can decide whether each pair is identical without assuming them to follow the normal distribution (nonparametric test). The null hypothesis (H_0) is that both populations (model output data) are the same and the alternate hypothesis (H_1) is that one particular model (LU or NLU) has greater values than the other.

4.6 Model comparissons

The scenario of this simulation is of loam soil, medium root length density, high potential transpiration and high initial concentration (Table 2). We compare all model

types (no solute uptake – NU; constant – CU; linear – LU and nonlinear – NLU concentration dependent uptake rates). All simulations were made until the value of relative transpiration was equal or less than 0.001. The time step is dynamical (depends on the number of iterations for water and solute equations) and was set to vary between 0.1 and 2 seconds. The simulation for NU ended within near 3 days; for CU, LU and NLU, about 5 days.

5 RESULTS AND DISCUSSION

The simulations were performed using the hydraulic parameters from the Dutch Staring series (WÖSTEN et al., 2001) for three typical top soils, as listed in Table 1. The general system parameters for the different scenarios are listed in Table 2 and values for the Michaelis-Menten (MM) parameters in Table 3. Values of root length density, salt content and relative transpiration were chosen to change, reflecting different possible scenarios that would occur in a practical situation. The chosen MM parameters were for K^+ solute.

Table 1 - Soil hydraulical parameters used in simulations

Staring soil ID	Textural class	Reference in this paper	θ_r $m^3 m^{-3}$	θ_s $m^3 m^{-3}$	α m^{-1}	l $-$	n $-$	K_s $m\,d^{-1}$
B3	Loamy sand	Sand	0.02	0.46	1.44	-0.215	1.534	0.1542
B11	Heavy clay	Clay	0.01	0.59	1.95	-5.901	1.109	0.0453
B13	Sandy loam	Loam	0.01	0.42	0.84	-1.497	1.441	0.1298

Source: Wösten et al. (2001)

Table 2 - System parameters used in simulations scenarios

Description	Symbol	Scenario description	Value	Unit
Root radius	r_0		0.5	mm
Limiting root potential	h_{lim}		-150	m
Root density	L	Low root density	0.01	cm cm^{-3}
		Medium root density	0.1	
		High root densit	1	
Half distance between roots	r_m	Low root density	56.5	mm
		Medium root density	17.8	
		High root densit	5.65	
Potential transpiration rate	T_p	Low	6	mm d^{-1}
		High	3	
Initial salt content in soil water	C_{ini}	Low	14	mol cm^{-3}
		High	140	
Diffusoin coefficient in water	$D_{m,w}$		1.98 10^{-9}	m^2 s^{-1}
Dispersivity	τ		0.0005	m
Soil type		Sand Clay Loam	Table 1	

Table 3 - Michaelis-Menten parameters after Roose and Kirk (2009)

Solute	I_m mol m^{-2} s^{-1}	K_m mol m^{-3}
NO_3^-	1 10^{-5}	0.05
K^+	2 10^{-6}	0.025
$H_2PO_4^-$	1 10^{-6}	0.005
Cd^{2+}	1 10^{-6}	1

5.1 Linear versus nonlinear comparison

In all simulated scenarios, the difference between LU and NLU models occurs only at values of solute concentration in soil water (C) below the threshold value C_{lim}. This is expected because of the nature of the piecewise MM equation used in the model. For both models, when solute concentration values are higher than C_2, solute transport from soil to root is mostly driven by convection, therefore the uptake is passive with active uptake equal to zero. For values of C between the two threshold values (C_2 and C_{lim}), the solute flux density is constant and NLU and LU are different only for C values lower than C_{lim} .

The absolute difference between C outputs of LU and NLU was calculated according to Equation (55). When comparing differences in concentration between the two models, one has to be aware that $CNL < CL$ means that the uptake for NLU is greater than LU uptake since with a higher uptake, a higher amount of solute goes out from soil solution to inside the plant. Therefore if $diff < 0$ then $CNL > CL$ and LU uptake is greater; if $diff > 0$ then $CNL < CL$ and NLU uptake is greater. Said that, we can see in Figure 8 that the uptake for NLU is greater then LU uptake at times when $C < C_{lim}$. This reflects a change also in the concentration profile for the latter times. Figure 9 shows the concentration profile at day 5 and the difference between CL and CNL through the profile. The higher NLU uptake increases the concentration gradient causing a higher solute flux (most diffusive since water flux is very small) from soil towards the root, resulting in a slightly higher concentration for NLU close to root surface ($diff. < 0$).
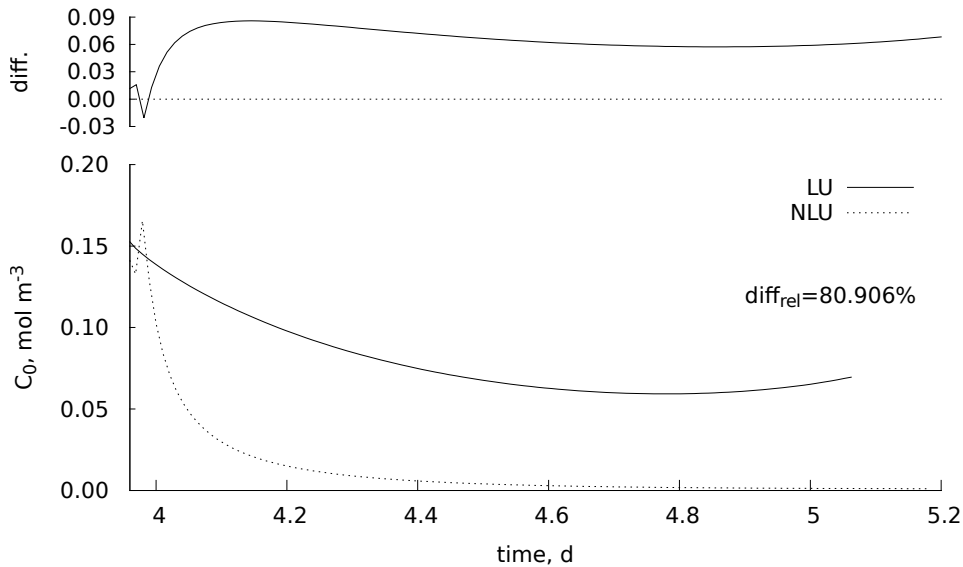

Figure 8 - Difference between the solute concentration in soil water at root surface (C_0) output for LU and NLU and C_0 as a function of time; and the relative difference – Scenario 1
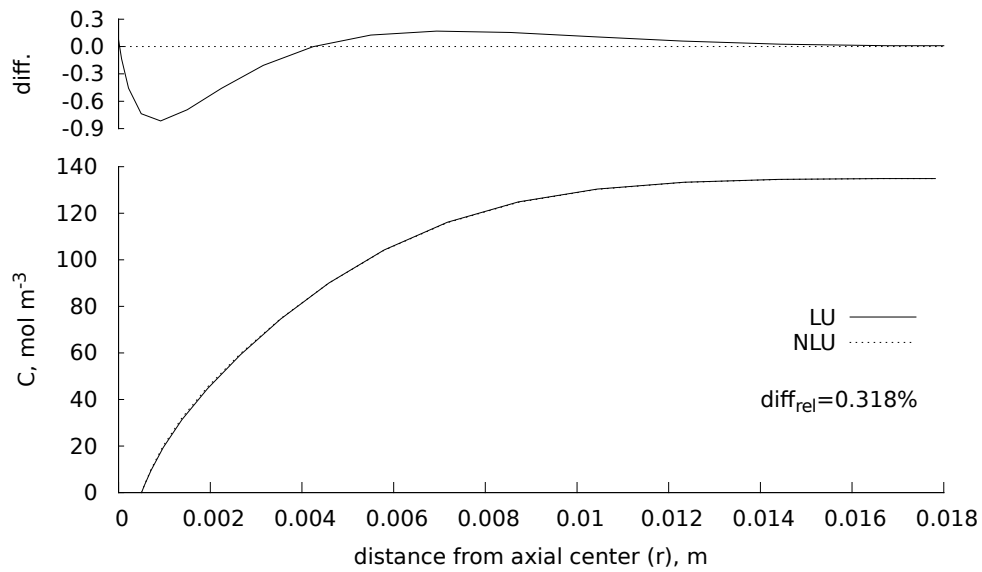
Figure 9 - Difference between the solute concentration in soil water (C) output for LU and NLU and C as a function of distance from axial center; and the relative difference – Scenario 1

The Mann–Whitney U test for (Table 4) shows that, for scenarios 1, 2 and 4, the differences between CL and CNL are significant for concentration values at times where $C < C_{lim}$ and, for scenario 3, both models have similar results. INCOMPLETE (in development)

Table 4 - Mann–Whitney U test p-values for all scenarios. * represents significant difference between LU and NLU for the given variable, with confidence interval of 95%

Scenarios	p-value concentration	p-value cum. uptake
1	$2.2 \ 10^{-16*}$	0.85
2	$1.5 \ 10^{-12*}$	0.86
3	0.14	0.99
4	$2.9 \ 10^{-16*}$	1.00

Nevertheless, the difference between LU and NLU is negligible for cumulative uptake. A difference of 80.9% of concentration over time (Figure 8) corresponds to only 0.318% in the final concentration profile (Figure 9) because the uptake at times where $C < C_{lim}$ is really low. It can be seen at the cumulative uptake plot (Figure 10) the insignificant effect of this difference (for both models, the cumulative solute uptake is nearly the same).

Similar to Figures 8 and 9, the results of the relative accumulated error, according to Equation (56), were of 64.975% and 0.739%; 37.364.3% and 0.041%; 36.144% and 0.027% over time and distance for scenarios 2, 3 and 4, respectively.
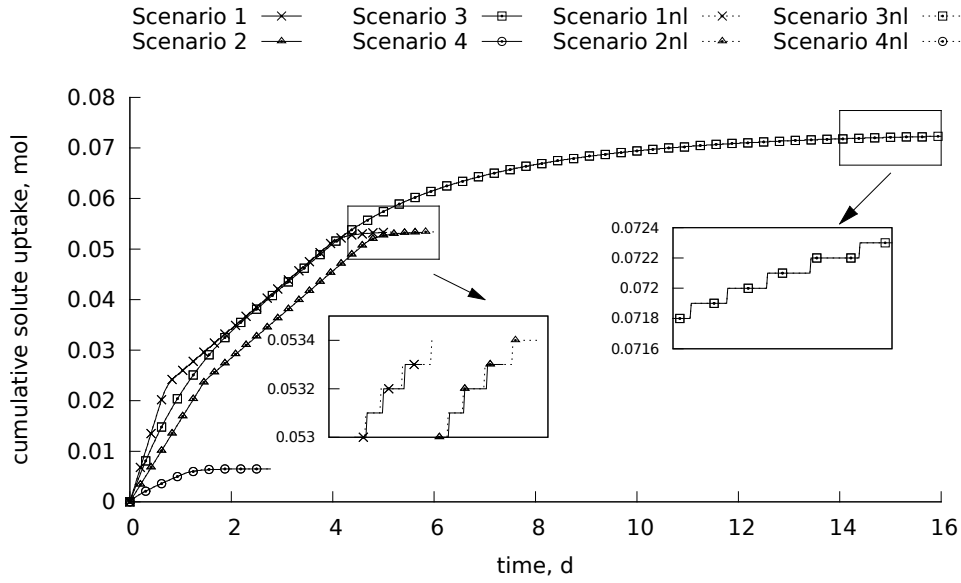
Figure 10 - Cumulative solute uptake as a function of time for all scenarios. Dashed lines represents the nonlinear model

In addition, some part of the differences was due to stability problems with the numerical solution for NLU. The changing from equation 21 to equation 25 (change of boundary condition, from constant to nonlinear uptake rate) makes the numerical solution take some time to stabilize at the initial times. Many time and space steps combinations were used as an attempt to minimize the problem. Choosing a finer space discretization seems to decrease the stabilization problem but makes the simulation lasts longer. It needs to be found an optimal value for time and space step relation. Stabilization problems were not found in LU.

Since the differences between LU and NLU occurs for low concentration values and low solute flux, changes in relative transpiration are also negligible. The oscillation in the results due to the stabilization problem of the numerical solution is more likely to be noticed than the difference between the models. Figure 11 shows the relative transpiration as a function of time and details the part where the oscillation occurs for each scenario. The absolute and relative differences are all due to oscillation problem, since T_r turns out to be the same after complete convergence.
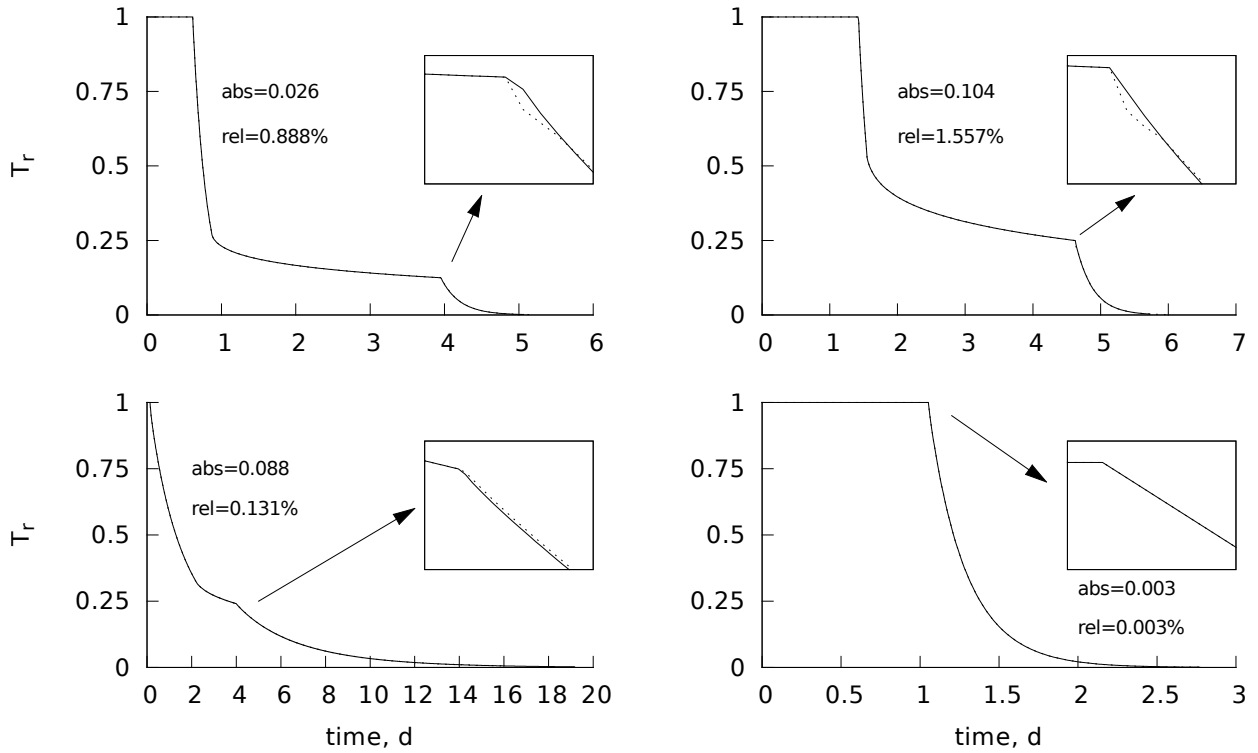
Figure 11 - Cumulative solute uptake as a function of time for all scenarios. Dashed lines represents the nonlinear model

Roose and Kirk (2009) stated that, for numerical solutions of convection-dispersion equation, the convective part might use an explicit scheme because convection, unlike diffusion, occurs only in one direction thus the solution at the following time step depends only on the values within the domain of influence of the previous time step. This set bounds on time and space steps, with a condition of stability given by $\frac{r_0 q_0 \Delta t}{D} < \Delta r$. As the proposed model uses a fully implicit scheme, that might be the cause of the stabilization problems.

The conclusion, since no significant difference between LU and NLU was found, can be either to choose LU as it takes less time to run and has no stabilization problems, or to choose NLU except for the cases in which the stability problem is significantly high. Note that this is the conclusion for those specific scenarios as the results can be significantly different for different soil and solute types.

5.2 Solute uptake models comparison

In NU, salt is transported to the roots by convection, causing an accumulation of solutes at root surface. As water flux towards the root starts to decrease, salt is transported slower and carried away from the roots by diffusion (Figure 12). Because of

the accumulation of salt in the root surface, the total head becomes limiting very fast and the transpiration is reduced faster than the other models (Figure 15).

In CU, as the salt uptake rate is constant (Figure 14), the concentration at root surface will decrease only if the uptake rate is larger than convection to the root surface. In the simulation, it happens in about half of the first day (Figure 12). This is very dependent on the uptake rate and water flux since for different conditions, the outcome could be different. Once the concentration at root surface is zero, the root behaves as a zero-sink, taking up solute at the same rate as which it arrives at the root, keeping the concentration there zero.

In NLU, the concentration at root surface remains constant (Figure 12) until the convection to the root decreases as the water flux decreases (Figure 14). This behavior is really dependent of initial concentration and water flux values since, in this case, C_0 at the beginning of simulation is greater than C_2, thus the solute uptake equals the convection of solutes to the root. At around day 1, convection starts to decrease but the solute uptake is yet greater than the plant demand (I_m) due to convection. The solute uptake becomes constant (and equal to I_m) after concentration in root surface is less than C_2. This is clear in XXXFigure 3a, where osmotic head continues constant for a period of time after the beginning of the falling transpiration rate. At this point, active uptake starts since convection only is not capable to maintain solute uptake rate at I_m. The concentration keeps decreasing at this constant rate until its value is less than C_{lim}. It is assumed that, at this point, the uptake is not equal to the plant demand for solute (I_m) due to the concentration dependence of the MM equation (Figure 7). The water flux and the concentration are small as well as the active uptake, that can not maintain the uptake rate at I_m. Therefore, a second limiting condition occurs when $C < C_{lim}$ causing another fast decrease in transpiration (Figure 15). The calculated concentrations C_{lim} (Eq. (25)) and C_2 (Eq. (27)) depend on water flux and ion type (MM parameters I_m and K_m) meaning that the results can be quite different for other ion types and different values of initial water content.

Figure 14 also shows the changes in solute flux at root surface for all models. At low concentrations (or at the second falling rate stage: $C < C_{lim}$), in NLU, the solute flux decreases gradually over time until the value of concentration is zero, where it will assume the zero-sink behavior.

The concentration profile through the distance from root axial center is shown in Figure 13. The different approaches (NU, CU and NLU) result in different final concentrations profiles. The concentration dependent model NLU takes up more solute from soil solution due to the higher uptake rate in the constant transpiration phase.

Figure 15 shows the relative transpiration as a function of time for the three model types. The proposed model is able to maintain the potential transpiration for a longer period of time due to the extraction by passive uptake only ($C > C_2$) that keeps the osmotic head constant, allowing pressure head to reach smaller values at the onset of the limiting hydraulic conditions, as can be seen in Figure 6.

Figure 15 shows that CU and NLU have a more negative pressure head value for the onset of limiting hydraulic condition when compared to NU due to solute uptake that causes a increase in osmotic head (becomes less negative) and, in turn, decreases pressure head. Thus, the first falling rate phase of relative transpiration extends in time. The solute uptake at the beginning of the simulation (for concentrations greater than C_2) caused a greater accumulation of solute in the plant and also influenced the final solute profile, in which LU and NLU have less solute left in the soil profile (Figure 13).

At the onset of the second falling rate phase ($C < C_{lim}$), water and solute fluxes decreases rapidly. In Figures XXX10 and 20 we can see that from day 4 to day 5, the fluxes are rapidly reduced, the water flux is near zero in the whole profile, meaning zero or really small convection. Thus, within this period, the transport of solute is made mainly by diffusion and the results of this diffusive transport can be visualized in Figures XXX17 and 18.
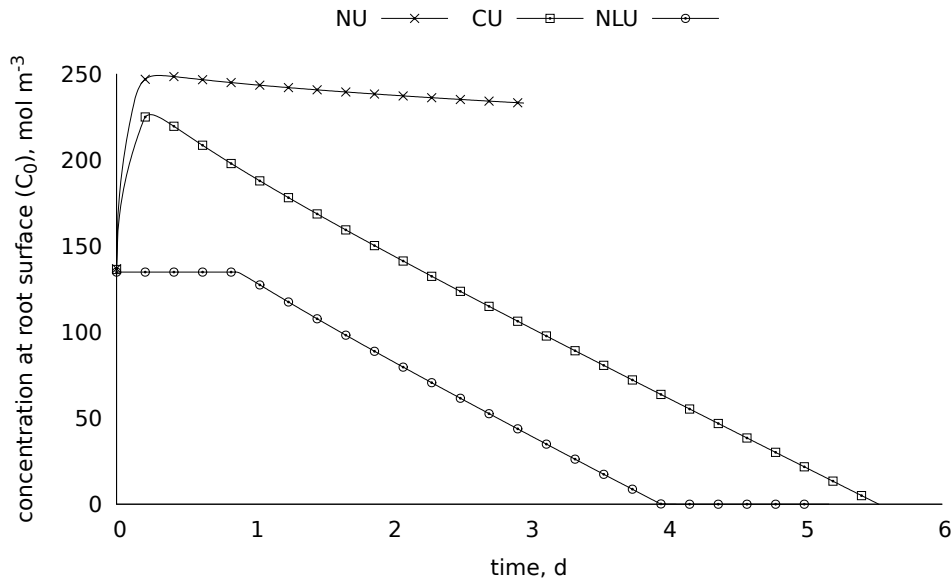
56

Figure 12 - Solute concentration in soil water at root surface as a function of time for no uptake (NU), constant (CU) and nonlinear (NLU) uptake models
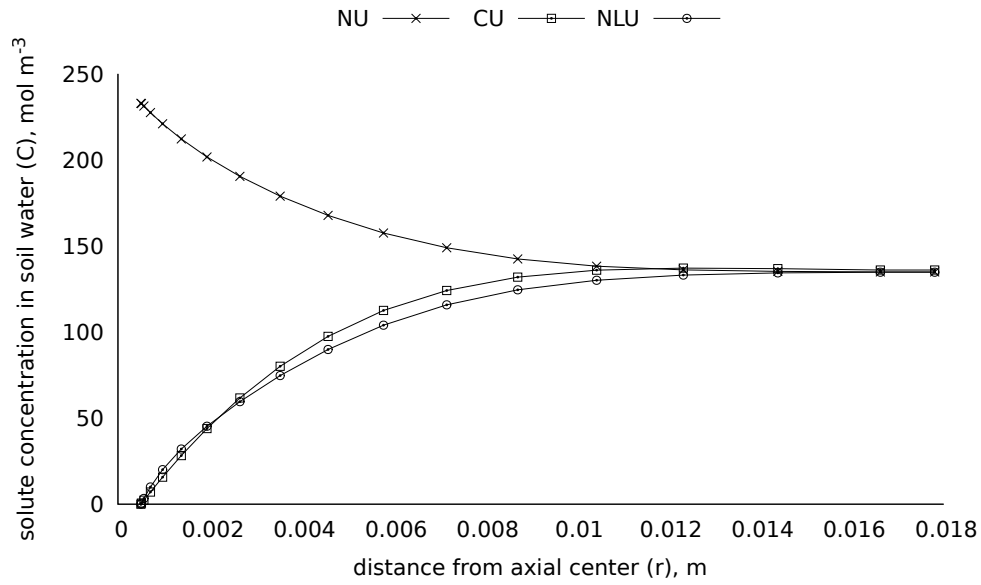
Figure 13 - Solute concentration in soil water as a function of distance from axial center for no uptake (NU), constant (CU) and nonlinear (NLU) uptake models
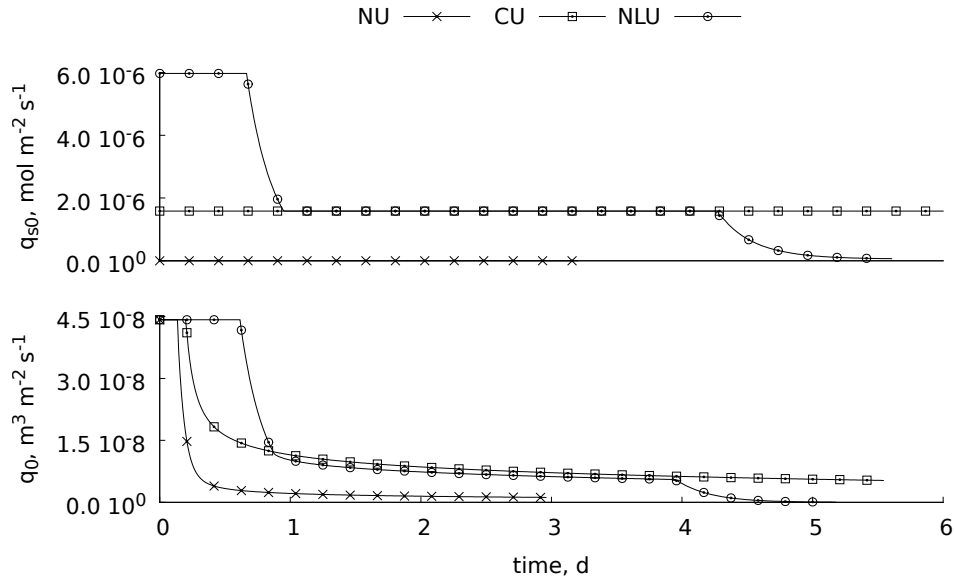

Figure 14 - Solute and water fluxes at root surface as a function of time for no uptake (NU), constant (CU) and nonlinear (NLU) uptake models
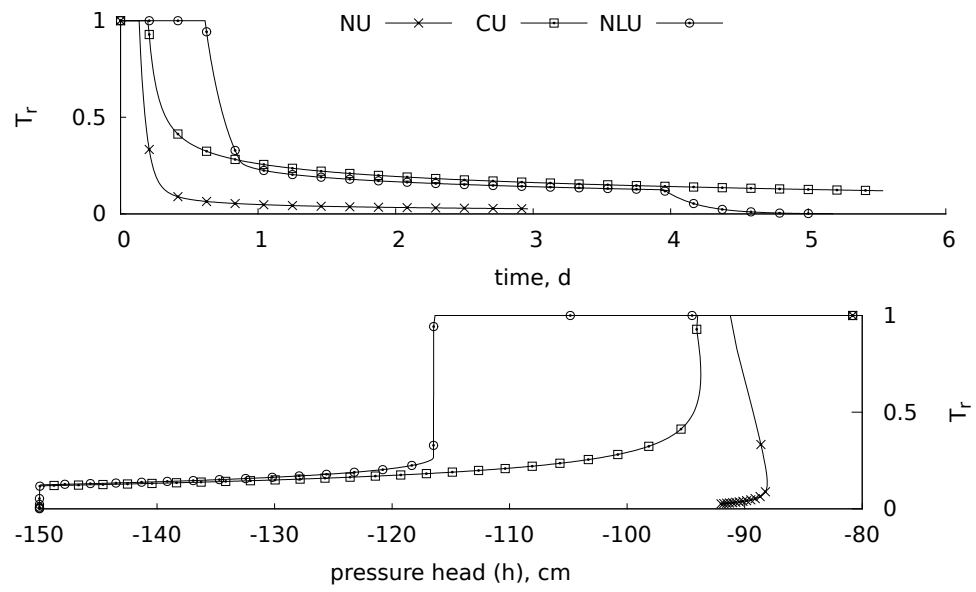
Figure 15 - Relative transpiration as a function of time and pressure head for no uptake (NU), constant (CU) and nonlinear (NLU) uptake models

6   CONCLUSION

The proposed model simulates the solute flux and root uptake considering a soil concentration dependent uptake. There was no significant difference between linear and nonlinear solutions for the simulated scenarios. The results of uptake for the proposed model showed that the limiting potential is reached at a higher pressure head, increasing the period of potential transpiration. It also showed a second limiting condition that happens at the time when $C < C_{lim}$ caused by a insufficient supply of solute at the same rate of plant demand. The proposed model is also able to do a partition between active and passive uptake which will be important to simulate the plant stress due to ionic or osmotic components, according to the solute concentration inside the plant. Comparison between the numerical and the analytical solution proposed by Cushman is in process.

REFERENCES

BARBER, S. Influence of the plant root on ion movement in soil. **Proc Plant Root Environ**, 1974.

BARBER, S.A. **Soil nutrient bioavailability: a mechanistic approach**. [S.l.]: John Wiley & Sons, 1995.

BECHTOLD, M.; VANDERBORGHT, J.; IPPISCH, O.; VEREECKEN, H. Efficient random walk particle tracking algorithm for advective-dispersive transport in media with discontinuous dispersion coefficients and water contents. **Water Resources Research**, Wiley Online Library, v. 47, n. 10, 2011.

BORSTLAP, A. The use of model-fitting in the interpretation of dual uptake isotherms. **Plant, Cell & Environment**, Wiley Online Library, v. 6, n. 5, p. 407–416, 1983.

BOULDIN, D. A multiple ion uptake model. **Journal of soil science**, Wiley Online Library, v. 40, n. 2, p. 309–319, 1989.

BROADLEY, M.R.; WHITE, P.J.; HAMMOND, J.P.; ZELKO, I.; LUX, A. Zinc in plants. **New Phytologist**, Wiley Online Library, v. 173, n. 4, p. 677–702, 2007.

DALTON, F.; RAATS, P.; GARDNER, W. Simultaneous uptake of water and solutes by plant roots. **Agronomy Journal**, American Society of Agronomy, v. 67, n. 3, p. 334–339, 1975.

DE JONG VAN LIER, Q.; METSELAAR, K.; VAN DAM, J.C. Root water extraction and limiting soil hydraulic conditions estimated by numerical simulation. **Vadose Zone Journal**, Soil Science Society, v. 5, n. 4, p. 1264–1277, 2006.

DE JONG VAN LIER, Q.; VAN DAM, J.C.; METSELAAR, K. Root water extraction under combined water and osmotic stress. **Soil Science Society of America Journal**, Soil Science Society, v. 73, n. 3, p. 862–875, 2009.

DUDAL, R.; DUDAL, R.; ROY, R. **Integrated Plant Nutrition Systems: Report of an Expert Consultation, Rome, Italy, 13-15 December 1993**. [S.l.]: Food & Agriculture Org., 1995.

EPSTEIN, E. Spaces, barriers, and ion carriers: ion absorption by plants. **American Journal of Botany**, JSTOR, p. 393–399, 1960.

EPSTEIN, E.; HAGEN, C. A kinetic study of the absorption of alkali cations by barley roots. **Plant physiology**, American Society of Plant Biologists, v. 27, n. 3, p. 457, 1952.

EPSTEIN, E. et al. **Mineral nutrition of plants: principles and perspectives.** [S.l.: s.n.], 1972.

FRIED, M.; SHAPIRO, R.E. Soil-plant relationships in ion uptake. **Annual Review of Plant Physiology**, Annual Reviews 4139 El Camino Way, PO Box 10139, Palo Alto, CA 94303-0139, USA, v. 12, n. 1, p. 91–112, 1961.

HILLEL, D. **Introduction to environmental soil physics**. [S.l.]: Academic press, 2003.

JOHNSON, K.A.; GOODY, R.S. The original michaelis constant: translation of the 1913 michaelis–menten paper. **Biochemistry**, ACS Publications, v. 50, n. 39, p. 8264–8269, 2011.

KELLY, J.; BARBER, S. Magnesium uptake kinetics in loblolly pine seedlings. **Plant and soil**, Springer, v. 134, n. 2, p. 227–232, 1991.

KOCHIAN, L.V.; LUCAS, W.J. Potassium transport in corn roots i. resolution of kinetics into a saturable and linear component. **Plant Physiology**, Am Soc Plant Biol, v. 70, n. 6, p. 1723–1731, 1982.

LAMBERS, H.; CHAPIN III, F.S.; PONS, T.L. **Plant water relations**. [S.l.]: Springer, 2008.

LIBARDI, P.L. **Dinâmica da Água no Solo Vol. 61**. [S.l.]: Edusp, 2005.

_____. água no solo. In: DE JONG VAN LIER, Q. (Ed.). **Física do solo**. Viccosa: Sociedade brasileira de ciências do solo, 2010.

LUX, A.; MARTINKA, M.; VACULÍK, M.; WHITE, P.J. Root responses to cadmium in the rhizosphere: a review. **Journal of Experimental Botany**, Soc Experiment Biol, v. 62, n. 1, p. 21–37, 2011.

MACHADO, C.T.d.T.; FURLANI, Â.M.C. Kinetics of phosphorus uptake and root morphology of local and improved varieties of maize. **Scientia Agricola**, SciELO Brasil, v. 61, n. 1, p. 69–76, 2004.

MARSCHNER, H.; MARSCHNER, P. **Marschner's mineral nutrition of higher plants**. [S.l.]: Academic press, 2012.

MICHAELIS, L.; MENTEN, M.L. Die kinetik der invertinwirkung. **Biochem. z**, v. 49, n. 333-369, p. 352, 1913.

MOUAT, M. Phosphate uptake from extended soil solutions by pasture plants. **New Zealand journal of agricultural research**, Taylor & Francis, v. 26, n. 4, p. 483–487, 1983.

NYE, P.; MARRIOTT, F. A theoretical study of the distribution of substances around roots resulting from simultaneous diffusion and mass flow. **Plant and Soil**, Springer, v. 30, n. 3, p. 459–472, 1969.

NYE, P.H.; TINKER, P.B. **Solute movement in the soil-root system**. [S.l.]: Univ of California Press, 1977. v. 4.

ROOSE, T.; FOWLER, A.; DARRAH, P. A mathematical model of plant nutrient uptake. **Journal of mathematical biology**, Springer, v. 42, n. 4, p. 347–360, 2001.

ROOSE, T.; KIRK, G. The solution of convection–diffusion equations for solute transport to plant roots. **Plant and soil**, Springer, v. 316, n. 1-2, p. 257–264, 2009.

SADANA, U.S.; SHARMA, P.; ORTIZ, N. C.; SAMAL, D.; CLAASSEN, N. Manganese uptake and mn efficiency of wheat cultivars are related to mn-uptake kinetics and root

growth. **Journal of Plant Nutrition and Soil Science**, Wiley Online Library, v. 168, n. 4, p. 581–589, 2005.

SEELING, B.; CLAASSEN, N. A method for determining michaelis-menten kinetic parameters of nutrient uptake for plants growing in soil. **Zeitschrift für Pflanzenernährung und Bodenkunde**, Wiley Online Library, v. 153, n. 5, p. 301–303, 1990.

SHI, J.; BEN-GAL, A.; YERMIYAHU, U.; WANG, L.; ZUO, Q. Characterizing root nitrogen uptake of wheat to simulate soil nitrogen dynamics. **Plant and soil**, Springer, v. 363, n. 1-2, p. 139–155, 2013.

SIDDIQI, M.Y.; GLASS, A.D.; RUTH, T.J.; RUFTY, T.W. Studies of the uptake of nitrate in barley i. kinetics of 13no3- influx. **Plant Physiology**, Am Soc Plant Biol, v. 93, n. 4, p. 1426–1432, 1990.

SILBERBUSH, M.; BEN-ASHER, J.; EPHRATH, J. A model for nutrient and water flow and their uptake by plants grown in a soilless culture. **Plant and soil**, Springer, v. 271, n. 1-2, p. 309–319, 2005.

ŠIMUNEK, J.; HOPMANS, J.W. Modeling compensated root water and nutrient uptake. **Ecological modelling**, Elsevier, v. 220, n. 4, p. 505–521, 2009.

TINKER, P.; NYE, P. **Solute Movement in the Rhizosphere**. Oxford University Press, 2000. (Topics in sustainable agronomy). ISBN 9780195124927. Disponível em: <http://books.google.com.br/books?id=I0D-nQEACAAJ>.

VALLEJO, A.J.; PERALTA, M.L.; SANTA-MARIA, G.E. Expression of potassium-transporter coding genes, and kinetics of rubidium uptake, along a longitudinal root axis. **Plant, Cell & Environment**, Wiley Online Library, v. 28, n. 7, p. 850–862, 2005.

WANG, M.Y.; SIDDIQI, M.Y.; RUTH, T.J.; GLASS, A.D. Ammonium uptake by rice roots (ii. kinetics of 13nh4+ influx across the plasmalemma). **Plant physiology**, Am Soc Plant Biol, v. 103, n. 4, p. 1259–1267, 1993.

WARRICK, A.W. **Soil water dynamics**. [S.l.]: Oxford University Press, 2003.

WILD, A. et al. Mass flow and diffusion. **The chemistry of soil processes**, p. 37–80, 1981.

WÖSTEN, J.; VEERMAN, G.; GROOT, W. D.; STOLTE, J. Waterretentie-en doorlatendheidskarakteristieken van boven-en ondergronden in nederland: de staringsreeks. Alterra, Research Instituut voor de Groene Ruimte, 2001.

APPENDICES

APPENDIX A - Finding C_{lim}

    CONTENT

APPENDIX B - Finding whether the solute flux for the linear model can be greater than from the nonlinear model

    The subscripts L and NL are relative to linear and nonlinear models, respectively. From Equations (31) and (32) we have:

$$q_{sL} = -(\alpha + q_{0L})C_{0L}$$
$$q_{sNL} = -\left(\frac{I_m}{(K_m + C_{0NL})} + q_{0NL}\right)C_{0NL}$$

We will check if there is any condition where $q_{sL} > q_{sNL}$. Then

$$(\alpha + q_{0L})C_{0L} > \left(\frac{I_m}{K_m + C_{0NL}} + q_{0NL}\right)C_{0NL} \tag{57}$$

    For Equation (57) to be true, there must exist at least one situation in which the inequality is true. From Equations (26) and (28), we know that:

$$\alpha = \beta - q_{0L} = \frac{I_m}{C_{limL}} - q_{0L} \tag{58}$$

Substituting Equation (58) into (57), we have:

$$\frac{I_m}{C_{limL}}C_{0L} > \left(\frac{I_m}{K_m + C_{0NL}} + q_{0NL}\right)C_{0NL} \tag{59}$$

    By knowing that the solute fluxes for linear and nonlinear models are different only for values of C_0 lower than C_{lim}, we can set the value of C_0 to C_{lim} and the equation is still valid. Thus:

$$\frac{I_m}{C_{limL}}C_{limL} > \left(\frac{I_m}{K_m + C_{limNL}} + q_{0NL}\right)C_{limNL}$$

With some algebraic operations, we have:

$$\frac{I_m}{C_{limNL}} > \left(\frac{I_m}{K_m + C_{limNL}} + q_{0NL}\right) \tag{60}$$

    Since I_m and K_m are constants and greater than zero, and C_{limNL} and q_{0NL} are also greater than zero, it can be easily seen that $\frac{I_m}{C_{limNL}}$ is always greater than $\frac{I_m}{K_m + C_{limNL}}$. Therefore, Equation (60) is true for all situations, except for the case:

$$q_{0NL} > \frac{I_m}{C_{limNL}} - \frac{I_m}{K_m + C_{limNL}}$$

Simplifying:

$$q_{0NL} > \frac{I_m K_m}{C_{limNL}(K_m + C_{limNL})} \tag{61}$$

We can solve Equation (61) for C_{limNL} to find the value in which the inequality is true:

$$C_{limNL}^2 + K_m C_{limNL} - \frac{I_m K_m}{q_{0NL}} > 0 \quad \Rightarrow \quad C_{limNL} > -\frac{K_m \pm \left(K_m{}^2 - 4\frac{I_m K_m}{q_{0NL}}\right)^{\frac{1}{2}}}{2} \tag{62}$$

Equation (62) is the same as Equation (25). Therefore, the condition (57) will never be satisfied since the affirmative $C_{limNL} > C_{limNL}$ is logicaly wrong.

It has been proved mathematically what was already possible to be noticed in Figure 7, that nonlinear uptake is always greater than linear and, therefore, that the linearization of the MM equation can be considered reasonable.